PROJECT PART-FINANCED BY THE EUROPEAN UNION

North East South West INTERREG IIIC

MATEO

MATEO ANTASME

ADVANCED MODELLING TECHNIQUES for AEROSPACE SMEs

DELIVERABLE 8.4 – "DEFINITION OF DATA INPUT AND OUTPUT STRUC-TURES FOR FUTURE IMPLEMENTATION IN GENERAL MULTIDISCIPLINARY CODES"

NOMENCLATURE

Variable	*Description*
A_r [m^2]	Radiator area
G [W/K]	Conductance
G_{back} [W/K]	Back conductance
H_{lv} [W/m^2 °C]	Evaporation enthalpy
H_{RL} [J/kg]	Specific enthalpy arriving from the liquid line
H_{RV} [J/kg]	Specific enthalpy transferred to the vapour line
$\dot{m}$ [kg/s]	Flow rate
Q_G [W]	Heat transfer between the vapour grooves and the evaporator wall
Q_W [W]	Heat transfer between the fluid wick with the solid one
Q_R [W]	Heat transfer between the two-phase reservoir with the solid one
Q_{WR} [W]	Heat transfer between the two-phase reservoir both with the solid wick
T [K]	Temperature
Uw [W/K]	Conductance inside the wick

Subscripts

Variable	*Description*
CC	Compensation chamber
Rad	Radiative
S	Steady state
Sat	Saturation

1 INTRODUCTION

Most thermal systems are generally rather complex and involving diverse physical processes. These last include natural and forced convection, radiation, complex geometries, property variation with temperature, nonlinearities and bifurcation, hydrodynamic instability, turbulence, multi-phase flows, or chemical reaction. It is common to have large uncertainties in the values of heat transfer coefficients, approximations due to using lumped parameters instead of distributed temperatures fields, or material properties that may not be accurately known. In this context, a complex system can be simplified with subsystems, each one can be singly analyzed and computed with accuracy and rapidity, but often when they are assembled in a global interconnected system present such a massive computational problem that are practically intractable. Most often some degree of approximation should be considered in the computational model. This could lead to consider a simplified model in which, for example, the main heat transfer processes are caught by using algebraic equations.
In this deliverable the LHP model is analyzed in order to obtain a simplified algebraic system able to reproduce the main output of the sinda/fluint model. Since the vapour and the liquid lines are adiabatic only the evaporator/reservoir and the condenser zone are considered The dataset of input and output structures reduces the LHP model to few objects useful for a future implementation in a multiphysics code.

1.1 Thermal analytic model

SINDA/FLUINT uses ad-hoc tools to simulate the evaporator/reservoir physical processes [1]. The heat transfers inside the evaporator are depicted in the next picture.

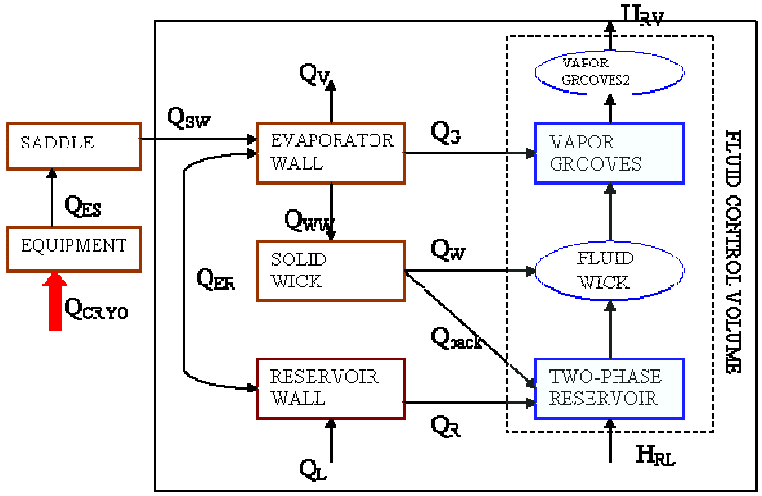

Fig. 1.1. Evaporator/reservoir heat transfer routes

The liquid control volume exchanges energy with the solid nodes through the link between the vapour grooves and the evaporator wall (Q_G), the fluid wick with the solid one (Q_W), the two-phase reservoir both with the solid one (Q_R) and with the solid wick (Q_{WR}). These powers have to balance the heat flux arriving from the liquid lines (H_{RL}) and transferred to the vapour line (H_{RV}):

$$\dot{Q}_G + \dot{Q}_W + \dot{Q}_{back} + \dot{Q}_R = (H_{RV} - H_{RL}) \cdot \dot{m} \qquad 1.1$$

In the steady state mode the overall power absorbed from the Cryo-Cooler comes in the evaporator wall ($\dot{Q}_{SW}$). Then, $\dot{Q}_{SW}$ crosses from the evaporator wall to the solid wick ($\dot{Q}_{SW} \approx \dot{Q}_{WW}$) and it is shared between $\dot{Q}_W$ and $\dot{Q}_{back}$. It is possible to explicit these two powers as functions of two conductances (the first inside the wick Uw, and the second one from the wick to the reservoir G_{back}) and the temperature difference between the solid wick and T_{sat} (ΔT):

$$\dot{Q}_{back} = G_{back} \cdot \Delta T \qquad \textbf{1.2}$$
$$\dot{Q}_W = U_W \cdot \Delta T$$
$$\dot{Q}_{back} / \dot{Q}_W = G_{back} / U_W$$

The liquid flow rate $\dot{m}$ depends on the power $\dot{Q}_W$ and the evaporation enthalpy at saturation temperature (T_{sat}):

$$\dot{m} = \frac{\dot{Q}_W}{H_{lv}(T_{sat})} \qquad \textbf{1.3}$$

Besides the pressure in the end of the liquid line (P_L) is close to the saturation pressure (P_{sat}) because the possible difference is due only to the pressure losses at the entrance in the reservoir from the liquid line.
By using the previous simplifications the Eq. (1.1) becomes:

$$\frac{G_{back}}{U_W} + 1 = \frac{H_{RV}(T_{CC}) - H_{RL}(T_S, P_{CC})}{H_{lv}(T_{CC})} \qquad \textbf{1.4}$$

Looking at Eq. (1.4), there are two parameters (G_{back}, U_W) and two unknown variables, so another equation is necessary. This equation comes from the energy balance in the condenser (Fig. 1.2):

$$(H_{RL}(T_S, P_{CC}) - H_{RV}(T_{CC})) \cdot \dot{m} = Q_{flux} - Q_{out} \qquad \textbf{1.5}$$

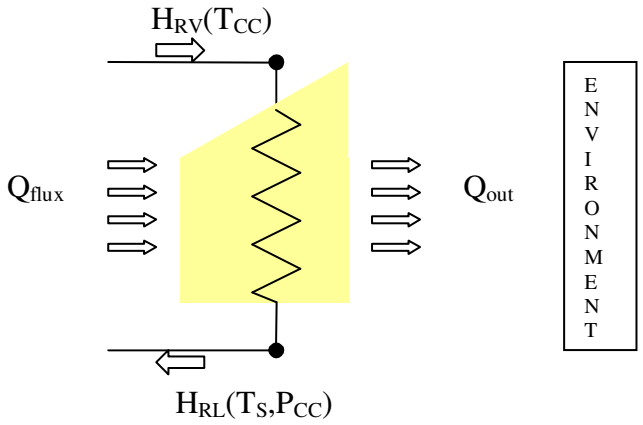

Fig. 1.2. Power balance in the radiator

The heat rate from the evaporator (H_{RV}) depends on the temperature and the pressure at the radiator inlet. By simple considerations these two properties are related to the corresponding two at the inlet of the vapour line. In fact because the line is adiabatic, the temperature changes depends only on the axial conductances along the evaporator wall and can be considered negligible (furthermore the pressure drop has a small influence on the enthalpy). Hence the heat rate incoming in the radiator is function of the saturation properties: $H_{RV}(T_{sat})$. The same considerations can be reserved for the liquid line so the heat rate in the end of the condenser is $H_{RV}(T_L, P_{sat})$.
The power rejected from the radiator (Q_{out}) is due to the radiation towards the external environment. A radiative conductance G_{rad}, a unique temperature for the radiator plate (T_{rad}) and for the environment (T_{sink}) are considered, hence eq. (1.5) become:

$$(\boldsymbol{H_{RL}}(\boldsymbol{T_S},\boldsymbol{P_{CC}})-\boldsymbol{H_{RV}}(\boldsymbol{T_{CC}}))\cdot\dot{\boldsymbol{m}}=\dot{\boldsymbol{Q}}_{\boldsymbol{flux}}-\boldsymbol{G_{rad}}\cdot\left(\boldsymbol{T_{rad}}^4-\boldsymbol{T}_{\sin\boldsymbol{k}}{}^4\right) \qquad \textbf{1.6}$$

Now considering the Eq. (1.4) and (1.5) with the (1.6) the three variables are T_{sat}, T_L, T_{rad}. An approximation for the T_{rad} is the simple arithmetic average between the inlet and outlet fluid temperature in the condenser: $T_{rad}=0.5\cdot(T_{Cout}+T_{Cin})$, hence:

$$\begin{cases}\dfrac{1}{U_{WB}}+1=\dfrac{\dot{H}_{RV}(T_{sat})-\dot{H}_{RL}(T_L,P_L)}{\dot{H}_{lv}(T_{sat})} \\ \left(\dot{H}_{RL}(T_L,P_{sat})-\dot{H}_{RV}(T_{sat})\right)\cdot\dfrac{U_{WB}}{1+U_{WB}}\cdot\dfrac{\dot{Q}_{SW}}{\dot{H}_{lv}(T_{sat})} \\ =\dot{Q}_{flux}-G_{rad}\left((0.5\cdot T_L+0.5\cdot T_{sat})^4-T_{\sin k}^4\right)\end{cases} \qquad \textbf{1.7}$$

where U_{wb} is the ratio between the conductances in the wick (U_w,G_{back}), and $\dot{Q}_{back}$ is given in function of the overall power by using Eq. (1.2): $\dot{Q}_{back}=\left(U_W/\left(G_{back}+U_W\right)\right)\cdot\dot{Q}_{SW}$.
The algebraic system (1.7) has now 5 parameters (U_{wb}, Q_{SW}, Q_{flux}, G_{rad}, T_{sink}) and three variables. It is possible to solve it by using an iterative procedure. The results are shown in the next figure for the steady state operating temperature, T_{ssot}, and the temperature at the condenser outlet, T_{Cout}.
The results are related to three boundary conditions: (a) Q_{flux}=70 [W], U_{wb}=25/3 (b) Q_{flux}=0 [W], U_{wb} =25/3 (c) Q_{flux}=70 [W], U_{wb}=25/6. For all the cases the radiative conductance G_{rad} is $5.0\cdot10^{-9}$ [W/T^4] and the T_{sink} is 170K.

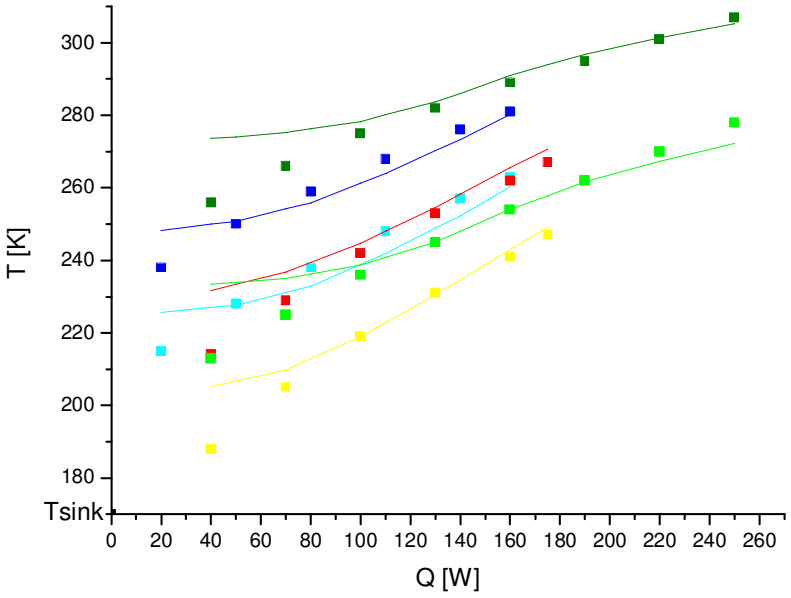

	T_{CC}, case (a)		T_{CC} from algebraic system, case (a)
	T_S, case (a)		T_S from algebraic system case (a)
	T_{CC}, case (b)		T_{CC} from algebraic system case (b)
	T_S, case (b)		T_S from algebraic system case (b)
	T_{CC} , case (c)		T_{CC} from algebraic system case (c)
	T_S, case (c)		T_S from algebraic system case (c)

Fig. 1.3. Temperatures in the LHP vs the overall heat power

The results show a good accordance when the power is increasing, while generally the system (1.7) defines LHP temperatures lower than the SINDA predictions for smaller values of the heat power. The approximation for the radiator temperature, T_{rad}, may be the reason of such discrepancy. Three different errors are due to this approximation:

1) The average is made between the fluid nodes at the condenser inlet and outlet so its value should be lower when the radial conductance in the pipe between the fluid and the radiator is considered.

2) The second error can be explained by looking at the LHP temperature profile in the condenser when the power inlet to the evaporator is high (Fig. 1.4).

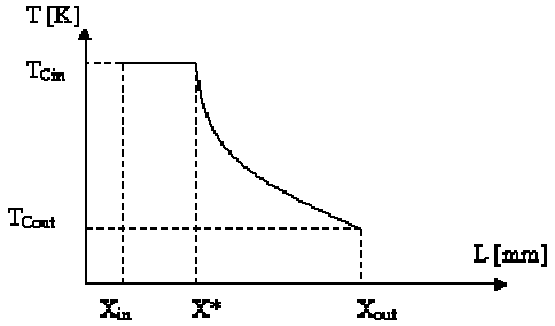

Fig. 1.4. Temperature profile in the condenser

The condenser is subdivided into two parts. The first (X_{in}-X*) in which the initial temperature is similar to the saturation temperature ($T_{Cin} \approx T_{sat}$) and the fluid is two-phase. The second

where only liquid is flowing and the temperature decreases towards T_{Cout}. The average between T_{Cin} and T_{Cout} is lower than the real temperature average ($1/Nc \cdot \sum T_C$; Nc= node number) in the condenser when the first part is long, i.e. when the power is high. This error leads to consider an greater value for the radiator temperature and may compensate the effect due to not considering the radial conductance in the pipe.
3) The third error can be explained by analyzing the SINDA/FLUINT simulations when the power is low. The resulting temperature profiles (depicted in Fig. 1.5) is different from the one showed in Fig. 1.4.

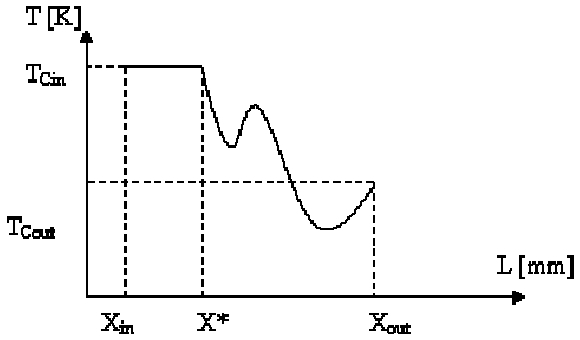

Fig. 1.5. Temperature profile in the condenser

It is evident the presence of two maximum. They are due to the design of the condenser in the zenith radiator (Fig. 1.6).

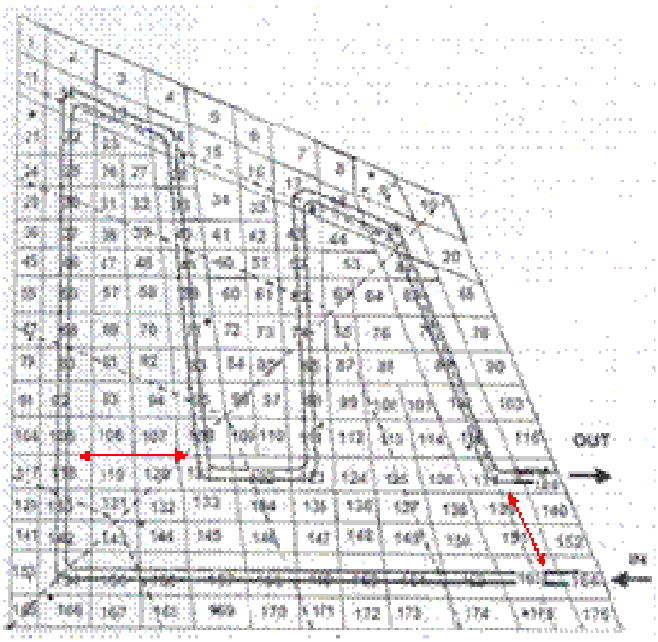

Fig. 1.6. Condenser design, the red arrows show the heat transfer between different parts of the condenser

The initial part of the pipe is near the end. The high temperature of the incoming two-phase fluid causes a important heat transfer (shown from the red arrow) to the outgoing fluid, the T_{Cout} increases and consequently the T_{ssop} is higher. Another heat flux is exchanged between two parts of the same condenser in the middle of the radiator (red arrow) and leads to the first maximum in figure Fig. 1.5.

1.2 Input/Output structures

The dynamic behaviour of any thermal system, schematically shown in Fig. 1.7, may be mathematically represented as:

$$L_0(y, x, u, w, \lambda) = 0 \qquad \textbf{1.8}$$

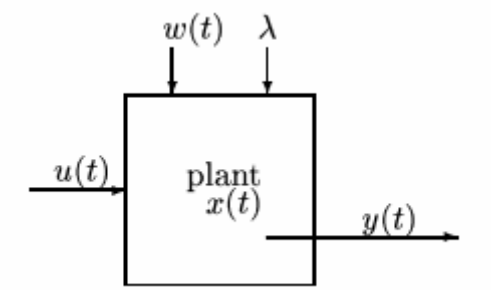

Fig. 1.7. Schematic of a dynamic sistem

Where $\mathcal{L}_o$ is a system operator, t is time, x(t) is the state of the system, u(t) is the input, w(t) is some external or internal disturbance, and λ is a parameter set which defines some characteristic of the system. Each one of these quantities belongs to a suitable set or vector space and there are a large number of possibilities.
Symbolically, the solver $\mathcal{L}_o$ could be either SINDA/FLUINT or the algebric system (1.7).
Therefore, in the latter case (Eq. 1.9) the output is constituted by a vector (**y**) that includes the steady state operating temperature and the temperature outcome from the condenser while the input includes the power coming in the evaporator (**u**). The "disturbances" (**w**) are constituted from the boundary conditions: the external fluxes in the radiator (Q_{flux}), the radiative conductance (G_{rad}) and the sink temperature for the radiator (T_{sink}). The parameters that define the system (**λ**) are both the radiator area (A_r) the ratio between the conductance inside the wick and the conductance from the wick to the reservoir (U_{WB}). This parameter is related to the geometry of the evaporator and it is assumed to be constant for every boundary conditions.

$$u = [Q]; \qquad \boldsymbol{w} = \begin{bmatrix} \boldsymbol{Q}_{flux} \\ \boldsymbol{G}_{rad} \\ \boldsymbol{T}_{\sin k} \end{bmatrix}; \qquad \lambda = \begin{bmatrix} A_r \\ U_{WB} \end{bmatrix}; \qquad y = \begin{bmatrix} T_{CC} \\ T_S \end{bmatrix} \qquad \textbf{1.9}$$

REFERENCE

1. Zinna S. & Marengo M. 2006 Simulation of the LHP in orbital conditions. *INTERREG IIICMATEO-ANTASME Deliverable 8.1.*